PAPER

Nanoscale spatial limitations of large-area substrate conformal imprint lithography

IOP Publishing Nanotechnology
Nanotechnology 30 (2019) 345301 (10pp) https://doi.org/10.1088/1361-6528/ab1c86

Nanoscale spatial limitations of large-area substrate conformal imprint lithography

M A Verschuuren[1,2], M W Knight[3,4], M Megens[1] and A Polman[3]

[1] Philips Research, High Tech Campus 4, 5656 AE Eindhoven, The Netherlands
[2] SCIL Nanoimprint Solutions, De Lismortel 31, 1612 AR Eindhoven, The Netherlands
[3] Center for Nanophotonics, AMOLF, Science Park 104, 1098 XG Amsterdam, The Netherlands
[4] Northrop Grumman Corporation NG Next, 1 Space Park Blvd, Redondo Beach, CA 90278 United States of America

E-mail: polman@amolf.nl

Received 18 December 2018, revised 12 April 2019
Accepted for publication 25 April 2019
Published 3 June 2019

Abstract

We demonstrate a soft-imprint nanofabrication technique offering nanometer resolution over an area as large as a 150 mm diameter wafer. It makes use of a composite imprint stamp composed of a quaternary siloxane-modified poly-di-methyl-siloxane patterned rubber layer with a relatively high Young's modulus that is laminated on a thin glass support. The in-plane stiffness of the stamp avoids pattern deformation over large areas, while out-of-plane flexibility allows conformal contact to be made over the entire substrate area. The stamp is used in conjunction with a novel tetra-methyl-ortho-siloxane/methyl-tri-methoxy-siloxane sol-gel imprint resist material developed to replicate nanoscale features in rigid silica at room temperature. We demonstrate better than 10 nm resolution in imprinted line gratings and individual pillars with aspect ratio as high as 5:1. Gaps as small as 6 nm can be reproduced. The patterns can be used as an etch mask to pattern 150 mm diameter silicon and quartz substrates while maintaining sub-10 nm resolution.

Keywords: nanoimprint, nanopatterning, soft-imprint, lithography, SCIL, soft imprint, large area

(Some figures may appear in colour only in the online journal)

1. Introduction

Nanoimprint lithography is a well-known replication technique by which patterns are transferred through an embossing principle [1–3]. It allows the high-throughput fabrication of three-dimensional nanostructures over large areas. Nanoimprint can enable the practical use of emerging nanotechnology designs in many application areas including solid-state lighting [4, 5], lasers [6, 7], sensors [8, 9] and photovoltaics [10–12]. The first demonstrations of nanoimprint lithography used rigid stamps to hot-emboss polymer layers [13] (NIL) or layers of UV-curable resists [14] (UV-NIL). These methods realized a resolution of 25 nm already in 1996 and have demonstrated patterns with feature sizes down to 5 nm [15]. NIL and UV-NIL promised a route to cost-effective fabrication of large-area nanostructures. However, the deployment of rigid-stamp nanoimprint technology has been hindered by the sensitivity of the contact between stamp and substrate to particle contaminants and wafer inhomogeneity. Additionally, releasing the rigid interlocking patterns requires substantial force that can damage the imprinted pattern or even the stamp itself.

Soft-nanoimprint lithography was simultaneously introduced as an alternative to imprinting with rigid stamps. Soft stamps proved more durable than rigid stamps and less sensitive to particle contaminants and wafer inhomogeneity. Additionally, multiple low-cost soft stamps can be replicated from a single master pattern. However, the resolution of soft-nanoimprint lithography has not previously been shown to match the performance of rigid stamp imprinting. This is due to nanoscale elastic deformation of the soft rubber features of the stamp. Although isolated, non-dense, nanoscale features can accurately be replicated using 'soft' stamps [16–19], this does not hold for dense nanoscale patterns,

such as gratings, which become unstable and collapse [20–28]. Furthermore, the low modulus of rubber stamps has thus far prohibited the accurate alignment and overlay of multiple layers.

Several combinations of rigid and soft stamp concepts have been previously studied with the aim to combine the benefits of rigid stamps (resolution) and soft stamps (large area). Soft stamps have been made on rigid supports to reduce pattern distortion over wafer scales, but these designs do not offer nanoscale resolution, as the features are molded in a low- modulus rubber that does not support dense nanoscale patterns. Thin rigid stamps have been made on soft and flexible supports to allow conformal contact over large areas [29, 30], but these designs remain vulnerable to particle contaminants that can cause damage to the stamp surface [31–33]. Other alternative composite stamps combining rigid and soft materials require high pressure or high temperature processing conditions, and do not allow for conformal contact, due to the high rigidity associated with the high modulus of the stamp material which holds the features [34]. A newly developed UV-curable fluoro-polymer has a relatively low modulus and is intrinsically non-stick [35]. However, this material must be used above its glass transition temperature, causing viscoelastic deformation, leading to deformation of the nanopatterns. Another technique, that uses a UV-curable stamp based on modified siloxane material, has demonstrated the replication of sub-100 nm features but requires the application of a separate anti-sticking layer, which will degrade and lead to stamp damage in the course of 25–150 imprint cycles [36].

Here, we present a new high-throughput wafer-scale Substrate Conformal Imprint Lithography (SCIL) method that addresses all of the challenges described above: this improved soft-stamp technique creates conformal, dense, high aspect ratio patterns using a method that is scalable from research laboratory to industrial scale. It can pattern full wafers, with diameters up to 200 nm, at once while creating dense and high aspect ratio sub-10 nm patterns. To attain nanometer resolution our method uses composite flexible large-area rubber stamps made from a quaternary siloxane-modified poly-di-methyl-siloxane (PDMS) material that is designed to have a high Young's modulus. This rubber is laminated to a thin glass carrier providing high in-plane stiffness while maintaining out-of-plane flexibility. We use this stamp to replicate patterns in a novel silica sol-gel based resist composed of tetra-methyl-ortho-silicate (TMOS) and methyl-tri-methoxy-silane (MTMS) that we have developed to minimize post-imprint shrinkage. The combination of the improved stiffness of the stamp rubber and the high silica content of the imprint resist leads to faithful replication of feature sizes smaller than 10 nm over a 150 mm diameter wafer. We demonstrate the versatility of SCIL through examples of dense, high aspect ratio nanoscale pattern replication in quartz and silicon over large areas with negligible pattern deformation.

2. Methods

2.1. PDMS rubber synthesis

The X-PDMS silicone rubber is made from a combination of vinyl-modified linear di-methyl-siloxanes (as in H-PDMS) and vinyl-modified quaternary siloxanes [37]. The mixture is cross linked with hydride modified linear siloxanes using a platinum catalyzed vinyl-hydride addition reaction. By changing the linear to quaternary siloxane ratio the Young's modulus can be tuned and a maximum Young's modulus of 80 MPa is obtained.

2.2. SCIL composite stamp fabrication

Before the rubber negative stamp is molded from the master pattern, the surface of the master is modified with a monolayer of 1,1,2,2-H-perfluoro-decyl-tri-chloro-silane through vapor phase deposition to prevent the possible adhesion of the X-PDMS material [38]. The X-PDMS components are thoroughly mixed and de-gassed and a 50 μm thick layer is formed over the master by spin coating for 30 s at 1000 rpm. This forms a tacky layer after a pre-cure for 15 min at 50 °C after which low-modulus PDMS (Sylgard 184) is poured over the X-PDMS layer on the master. This PDMS is squeezed between the master and a 200 μm thick AF45 glass support plate to form a uniform layer of ~0.5 mm thickness. The 'master—X-PDMS—PDMS—glass' sandwich is cured for 24 h in an oven at 50 °C. The rubber negative stamp is then released from the master by gentle peeling and excess PDMS protruding above the pattern plane is trimmed. Using this procedure we have demonstrated up to 45 stamps can be molded from the master without reapplication of the fluor monolayer or pattern degradation.

2.3. Sol-gel imprint resist synthesis

The sol-gel resist precursor developed in this work is prepared from tetra-methoxy-ortho-silicate (TMOS) and methyl-tri-methoxy-silane (MTMS) in a 1:1 molar ratio. This mixture is hydrolyzed for 30 min at room temperature using a 1:1 molar ratio of alkoxide-groups:water (the water is acidified with 1 M formic acid). After the hydrolysis reaction additional water is added to obtain a 9:1 total molar ratio of water:silicon. The hydrolyzed mixture is then stabilized by dilution with n-propanol to reach a concentration of 0.78 mol Si/kg and stored at −20 °C. The final sol-gel imprint resist material is prepared by mixing equal masses of the n-propanol diluted precursor and 1 weight-percent 1,2-propanediol.

3. High-resolution substrate-conformal imprint lithography in silica sol-gel resist

In soft-nanoimprint lithography, a rubber negative stamp is first molded from a master pattern that is typically generated using conventional electron-beam-, ion-beam-, or interference-lithography. The bulk stamp rubber must be sufficiently soft (Young's modulus $E \ll 1$ GPa) to enable

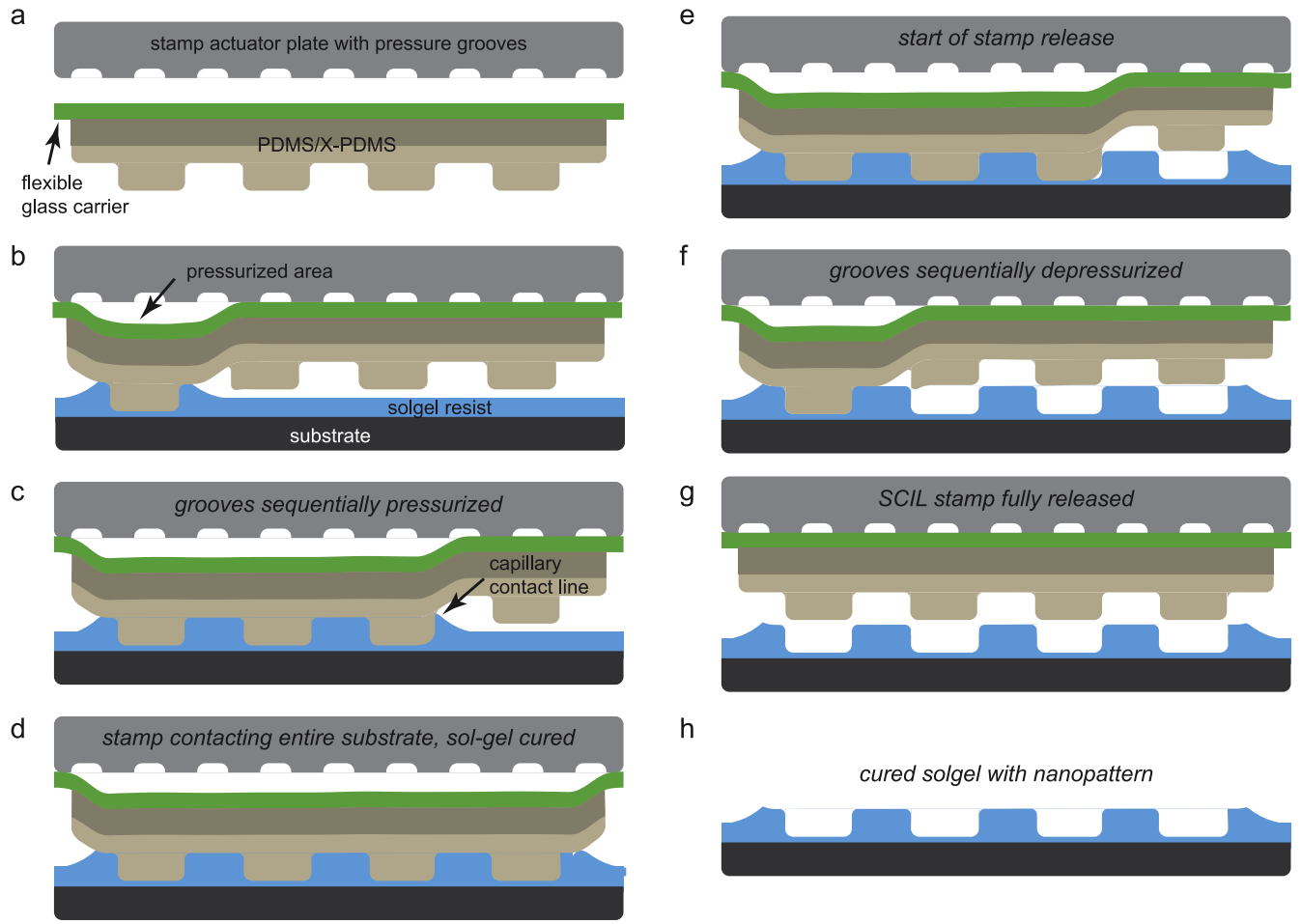

Figure 1. Large-area substrate-conformal imprint lithography (SCIL) principle. A rubber composite stamp is imprinted into a substrate covered with a liquid resist layer by sequentially pressurizing an array of grooves in the stamp actuator plate. Low imprint pressure is used and minimal force is required for release by peeling. Time sequence of an imprint step showing the evolution of the contact area by the sequential pressurization of the grooves (a)–(d) and after resist curing sequential release of the stamp (e)–(h). For clarity in visualization, illustration is not drawn to scale.

conformal contact over large areas. Silicone-based poly-di-methyl-siloxane (PDMS) rubbers are most commonly employed as they are chemically inert, have low surface energy, and have a high permeability for gases and solvents. Additionally these materials are non-toxic, biocompatible, and optically transparent to visible light. However, silicone rubbers typically have a low Young's modulus (1–3 MPa) which causes collapse of the stamp features at micrometer scales. To solve this problem a silicone rubber with a higher modulus (8 MPa) (H-PDMS) was previously developed, which allowed patterning down to ~200 nm scales before feature collapse occurred [21, 22]. Further improvement in the resolution of soft-nanoimprint lithography requires the development of new rubber materials with tunable increased stiffness. However, so far, the highest reported Young's modulus of a silicone rubber that is composed of combinations of linear siloxanes has been limited to 12 MPa. This material requires a curing temperature of 150 °C, which leads to high thermally induced pattern deformations [39].

To realize a stamp material with higher Young's modulus we have developed a material based on vinyl-modified quaternary siloxanes to increase the intrinsic cross-link density of the rubber [37]. The resulting silicone rubbers (X-PDMS) reach a Young's modulus up to 80 MPa. As a result, faithful replication of dense sub-10 nm features is possible, while still providing conformal contact over a full wafer, as will be demonstrated here. The X-PDMS is non-stick, has a low surface energy and can be directly used to pattern imprint resists, similar to commercial PDMS.

A SCIL composite stamp consists of a 200 μm thin glass sheet, a soft PDMS layer of ~0.5 mm thickness and a ~50 μm thick layer of X-PDMS that holds the nanopatterns. Our stamp replication method ensures that the rubber stamp is always attached to a mechanically stable carrier with high in-plane stiffness to maintain pattern fidelity. The out-of-plane flexibility of the thin glass support plate allows for substrate inhomogeneity and enables wafer-scale conformal contact, while the soft PDMS rubber layer allows local conformation around particle contaminants and thereby avoids damage to either the stamp or substrate.

Wafer-scale imprints are made using the composite stamps and a specially designed SCIL imprint tool. The stamp is held in the imprint tool by a 200 mm square flat plate with 80 grooves under low vacuum as shown in figure 1(a). The

substrate to be patterned is coated with a liquid sol-gel resist and aligned in the imprint tool parallel to the stamp at an initial spacing of ~100 μm. The stamp is then brought into contact with the substrate by sequentially pressurizing the grooves to an overpressure of ~20 mbar, starting from the side figures 1(b)–(d). This procedure gently curves the composite stamp over a length of ~2 cm until a line contact forms with the substrate. As the remaining grooves are sequentially pressurized to release the stamp, capillary forces pull the stamp into the resist and the line contact continually moves forward while avoiding air inclusions, as shown in figures 1(c), (d). The stamp is kept in contact while the liquid resist cross-links to form a solid silica replica. The composite stamp is then released from the patterned resist by sequentially evacuating grooves from one side, resulting in a controlled peeling-like release from the imprinted patterns figures 1(e)–(h). Because the stamp is gently rolled onto the sample surface (leading to temporarily 1D deformation) and then left to relax, pattern deformation is minimized, in contrast to some other techniques where the stamp is deformed in two dimensions by a high-pressure air cushion to make the stamp bulge out and contact the substrate [40, 41].

The sol-gel resist developed in this work consists of ~2.5 weight-percent pre-polymerized tetra-methoxy-ortho-silicate (TMOS) and methyl-tri-methoxy-silane (MTMS) in an alcohol/water mixture that contains 1 weight-percent 1,2-propanediol. Resist layers with a thickness ranging from 10 to 200 nm are formed by spin coating. Volatile components evaporate during the drying of the resist, leaving mainly silicon oxide oligomers and non-volatile 1,2-propanediol. The remaining 1,2-propandiol keeps the sol-gel liquid after spin coating during the ~1 min transfer of the substrate to the SCIL imprint tool. When the composite stamp is in contact with the substrate, 1,2-propanediol diffuses into the PDMS rubber stamp, which increases the concentration of reactive silicon-hydroxyl and silicon-alkoxide groups. These subsequently condense to form an inorganic network of Si-O-Si bonds while the reaction products (water and alcohols) are removed by diffusion into the stamp. After 3 min of contact at room temperature, the stamp can be removed from the glass sol-gel structure. The resulting sol-gel patterns are composed of ~90 weight-percent silicon oxide and remaining organic components. The solvents and reaction products from a 100 nm thick sol-gel layer are easily absorbed by the stamp. We did not experience effects of stamp saturation, even after more than 200 consecutive imprints.

Figure 2(a) shows scanning electron microscopy (SEM) images of imprinted silica gratings of 150 nm pitch, 25 nm width and 100 nm height on a silicon substrate. This demonstrates that high aspect ratio nanoscale features can be made directly using the X-PDMS stamp material. Similar structures would be impossible to fabricate directly using conventional (H-)PDMS due to collapse and sticking of the grating lines. Figure 2(b) shows silica pillars with a diameter of 130 nm and a height of 650 nm, demonstrating that individual high aspect ratio features can be printed with high fidelity. The high aspect ratio structures are reliably replicated as the voids in the stamp are rapidly filled with imprint resist by capillary forces while air trapped in the features diffuses into the rubber of the stamp. During release, the rubber stamp will temporarily deform to accommodate the release of the cured, rigid silica structures. These replicated patterns demonstrate that our high-Young's modulus X-PDMS silicone rubber is capable of faithfully replicating dense and high aspect ratio features. The images in figure 2 demonstrate faithful replication of patterns with a high surface-to-volume ratio.

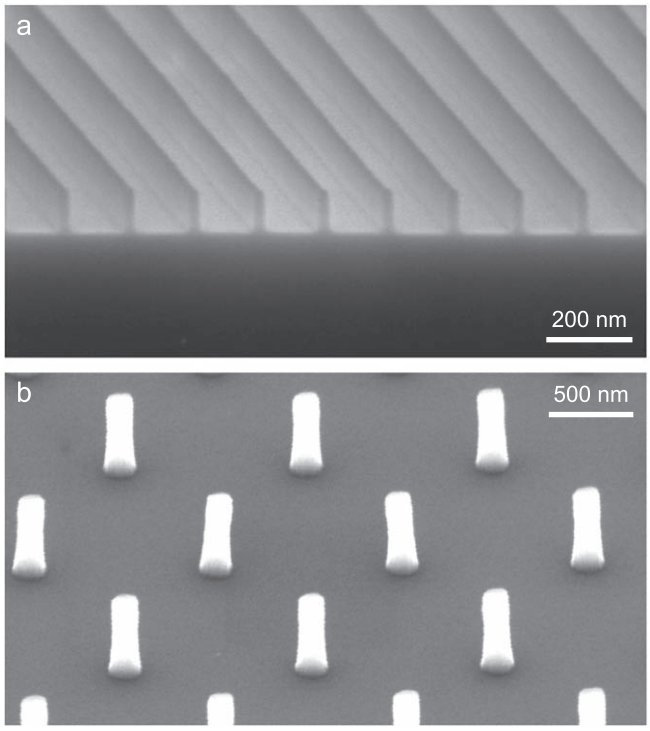

Figure 2. Directly replicated high aspect ratio patterns in silica. SEM images of (a) silica grating with 25 nm wide, 100 nm high lines at a pitch of 150 nm (image taken 10° out of plane); (b) silica pillars, diameter 130 nm, height 650 nm.

A single composite rubber stamp containing sub-50 nm lines was used to make over 700 imprints on 200 mm wafers in the sol-gel resist, with subsequent analysis confirming that patterns retained their shape to within +/−1 nm in width [42]. We did not observe any significant variation in the replicated patterns (height, width, shape) over the course of this experiment, confirming the durability of the inexpensive rubber stamp. Curing can be accelerated by chemically sensitizing the sol-gel resist to ultraviolet illumination, although the UV exposure does reduce stamp lifetime. For UV activated sol-gel resist the stamp lifetime is about 100 imprints, while for organic UV curable materials it is about 75 imprints [43, 44]. The direct patterning of light- and temperature-stable silicon oxide could be useful for IR, optical, and UV components such as gratings, photonic crystals, diffractive optical elements, graded index coatings, and templates for bit-patterned-media.

To study the pattern distortion over a large area we measured the variations in the pitch of a grating replicated using SCIL on a 150 mm diameter wafer. A 3 μm pitch master grating was made in a Si wafer using optical lithography and reactive ion etching (RIE); grating areas of 15 × 15 mm were stitched to populate the entire wafer. Next, a composite stamp was prepared as described above from the silicon master.

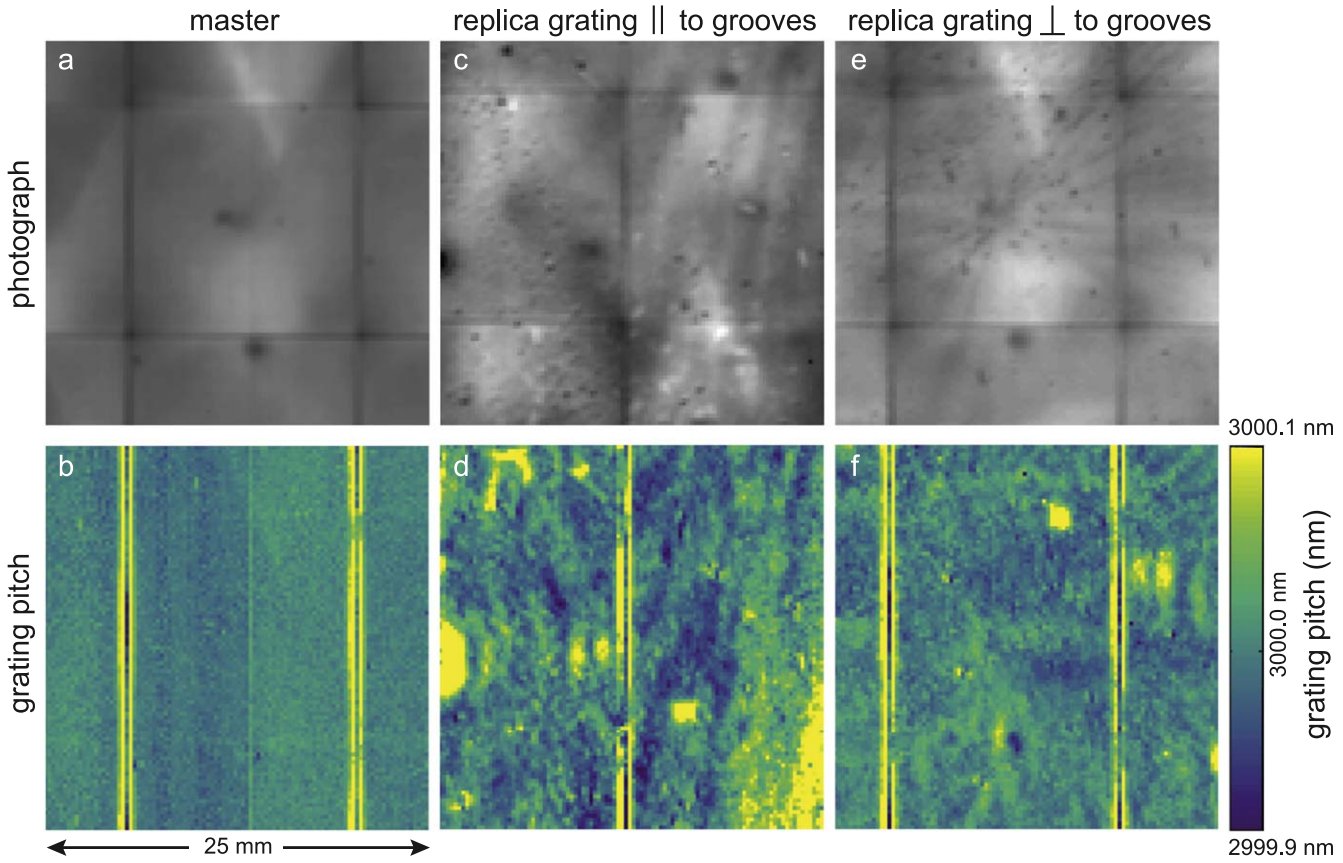

Figure 3. Ultra-small average pitch variation over large areas. Two-dimensional representations of pitch distributions for a silicon master and two SCIL replicated silica gratings imprinted on a Si substrate. The grating pitch is derived from diffraction angle measurements using a HeNe laser (spot size 125 μm). Photographs of the gratings and the associated measured grating pitches are shown for the master pattern (a)–(b) and sol-gel replicas imprinted either (c)–(d) parallel to the grating orientation or (e)–(f) perpendicular. The bright vertical lines are due to stitching errors between the 15 × 15 mm grating areas, introduced in the mastering process.

Using SCIL the grating was replicated in sol-gel on AF 45 glass substrates. The pitch of the master and sol-gel replica grating was determined by illuminating the grating perpendicular to the surface using a He-Ne laser at a wavelength of 632.8 nm with a spot diameter of 125 μm by measuring the variation in the angle between the reflected −4th and +4th diffraction orders using two CCD cameras (grating pitch resolution: 0.03 nm). By scanning the laser spot over the sample and tracking the reflected diffraction orders on the two cameras to measure the diffraction angle, we produced a two-dimensional map of the grating pitch averaged over the beam spot size. Figure 3 shows images of the grating pitch for the master (a) and the sol-gel replica, when the imprint direction (see figure 1) is applied parallel (b) or perpendicular (c) to the grooves in the SCIL actuation plate. As can be seen from the figure, the variation in average grating pitch (measured over the 125 μm spot size) for both the master grating and the replica grating is less than 0.1 nm. By comparing the images for the two imprint directions we conclude that the imprint direction does not influence the deformation of the replicated grating. The stepwise mechanical application of the stamp in the SCIL imprint tool does not lead to observable discontinuities in the pattern. The demonstrated average pitch variation of less than 0.1 nm over a 25 × 25 mm^2 area represents a very high replication fidelity [45, 46], which is fully attributed to the in-plane stiffness of the glass support of the PDMS layers. Printing these high-fidelity nanopatterns on active semiconductor materials enables the realization of polarization-controlled LEDs or lasers[47] as well as photonic crystals [48].

To show that low aspect ratio structures can also be replicated using SCIL, figure 4 shows white-light surface profilometry measurements of replicated gratings with a very low aspect ratio. Imprinting such structures is non-trivial as material has to flow and undergo transport over >100 microns through a sub-100 nm high channel which leads to squeezed flow and a reduced mass transfer speed. Structures with pitches of 128 and 256 μm were imprinted in a sol-gel imprint resist layer of only 100 nm thickness, leading to patterns with a height of 100 nm (note the different horizontal and vertical scale bars in figure 4). Line scans are taken perpendicularly to the grating lines. In figure 4(a) the raised areas of the 128 μm pitch grating are flat to within 2 nm while the recessed areas are flat to within 7 nm. The difference in flatness between the two levels can be explained by the more constricted material flow between the substrate and stamp in the recessed regions (sol-gel thickness 50 nm) and the raised areas (sol-gel thickness 150 nm). In figure 4(b), 256 μm pitch grating patterns are shown to be level to within only 40 nm. We attribute this to the onset of the gel state of the resist before the material flow has equilibrated. During the imprint

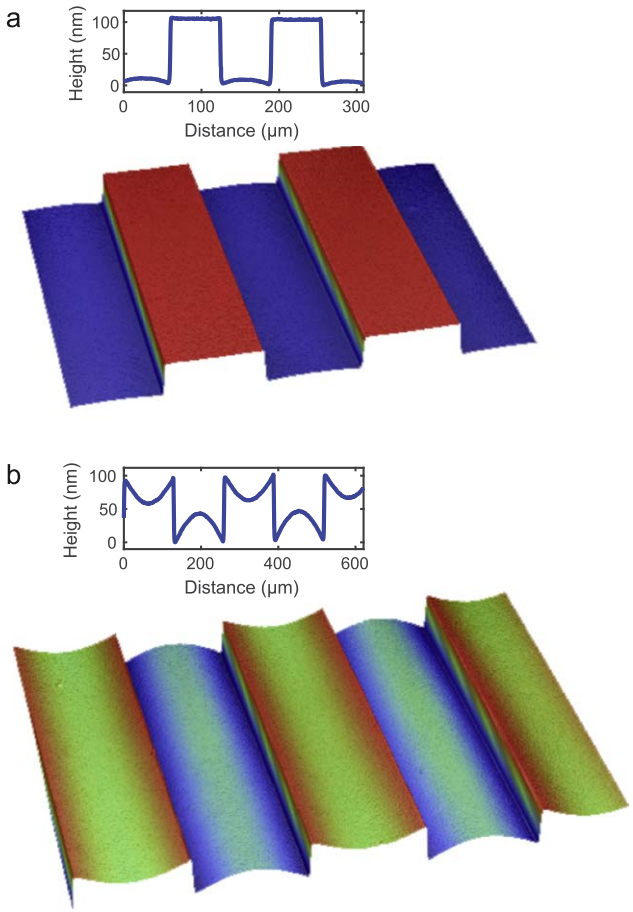

Figure 4. Very low aspect ratio gratings prepared by SCIL. White light interferometry surface profile of 100 nm high gratings with a pitch of (a) 128 μm and (b) 256 μm meter replicated in a 100 nm thick sol-gel layer. Line scans are shown taken perpendicular to the grating lines. Note the scale difference for the vertical and horizontal axes.

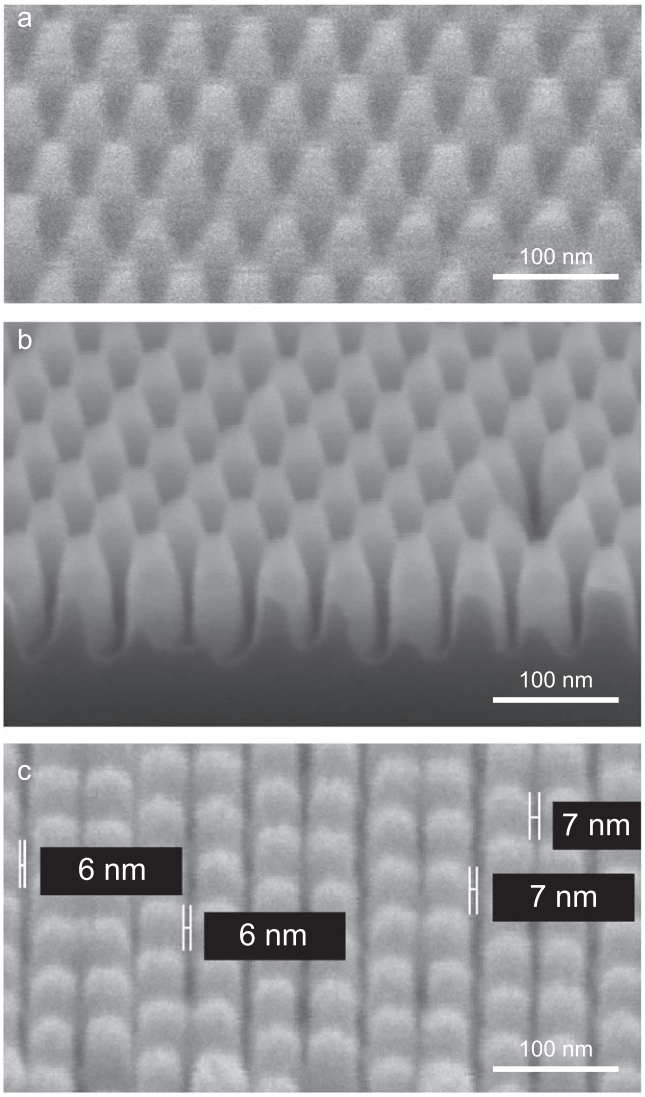

Figure 5. SCIL imprinted hard mask: 50 nm pitch pillars etched in silicon and quartz. (a) Image of the original etched fused silica master used to make the SCIL stamp. Contrast in the SEM image is low since no charge dissipation coatings were applied. Imprints on Si and quartz substrates were made using this pattern, followed by the removal of the ~20 nm thick residual sol-gel layer by a CF_4 RIE (b) The sol-gel mask was used to etch pillars into the underlying Si substrate using Cl_2/N_2 RIE; the oxide etch mask can be seen on top of the silicon pillars. (c) The sol-gel pattern was used to pattern a 6 nm thick chrome layer, after which the pattern was transferred into quartz using CHF_3/O2 RIE.

process, we observed that the gratings were index-matched when the stamp was in contact with the resist, indicating that the gratings were in complete contact with the liquid resist. This implies that capillary pressure is high enough to distort the rubber, leading to the observed curved pattern. This demonstrates that the capillary action of the resist is strong enough to successfully mold both high and low aspect ratio features, and high external imprint pressures are not required.

Previous work on the direct patterning of sol-gel materials reported volume shrinkages in excess of 10% at room temperature, resulting in deformed features after stamp release [49–51]. In this work, the combination of MTMS and TMOS led to a controlled reduction of the cross-link density in our imprint resist material. This allowed us to maximize the amount of inorganic silica in the liquid sol-gel during patterning and greatly reduce post-imprinting shrinkage. As a result, the replicated patterns are an exact, inverted copy of the stamp. We compared the dimensions of grating patterns immediately after imprinting and after sintering at 1100 °C to completely convert the sol-gel to dense silica (as confirmed by ellipsometry on planar layers). Even after sintering at these high temperatures the grating patterns such as in figure 2(a) are preserved, with a shrinkage of only 16% in width and 18% in height. From this feature shrinkage, we deduce that the initial sol-gel density is 70% when formed at room temperature, which is comparatively high for materials formed by a sol-gel route.

4. High-resolution pattern transfer in Si and SiO_2 and Cr

Due to the relative inertness of silica, an imprinted sol-gel pattern is an ideal hard mask to transfer patterns into a

substrate using RIE. After optimizing the initial resist layer thickness, the residual layer remaining under the recessed features after imprinting is typically <10 nm. This thin layer is removed using a fluorine RIE-based breakthrough etch. We achieve a highly anisotropic etch of the sol-gel material at a rate of 30 nm min^{-1} using CF_4 and N_2 in a 1:2 flow ratio at a pressure of 12 mTorr and a RF-power of 50 W. After the breakthrough etch, the underlying layer between the imprinted sol-gel features is exposed. This layer can subsequently be patterned by further etch steps. Figure 5 shows SEM images of a 50-nm-pitch fused silica master pattern (a), along with imprinted sol-gel patterns after transfer by etching into (b) silicon and (c) quartz. The silicon was etched to a depth of ~75 nm using a Cl_2/N_2 gas mixture at 40 mTorr and a RF-power of 100 W. The remaining sol-gel etch mask can be seen on top of the silicon pillars. To transfer imprinted patterns into quartz a 10 nm thick chromium transfer layer was first deposited on the quartz substrate wafer by sputter deposition. The sol-gel patterns were replicated on top of the chromium layer and the residual sol-gel layer was removed by fluorine RIE. A Cl_2/O_2 RIE process is used to pattern the chromium layer and a subsequent CHF_3/O_2 based RIE etch transfers the pattern to a depth of 100 nm into the quartz substrate (removing the sol-gel etch mask as well). Note that the gaps between the etched quartz pillars in figure 5(c) are as small as 6 nm, demonstrating that nanoscale features can be patterned with a SCIL mask, and subsequently transferred into a quartz substrate.

The uniformity of the residual resist layer thickness enables a reliable transfer of the imprinted features into the underlying layer during RIE over a large area. Using optical interference lithography a master pattern was made on a 150 mm diameter silicon wafer consisting of 360–375 nm diameter holes with a depth of 180 nm, on a square lattice with a pitch of 513 nm. Using the SCIL process, this pattern was replicated in sol-gel on a 150 mm diameter silicon wafer. A fluorine breakthrough etch removed 25 nm sol-gel material to expose the underlying silicon substrate. Subsequently a Cl_2/N_2 based RIE at a pressure of 40 mT for was used to transfer the hole pattern to a depth of ~260 nm into the silicon. The sol-gel etch mask was then removed in diluted HF. Figure 6 shows photographs of (a) the wafer with master hole pattern, (b) the SCIL composite stamp containing pillars and (c) the replicated hole pattern after etching into the silicon wafer and removing the sol-gel resist. The homogeneous interference colors seen in the photograph reveal that the pattern is homogeneously transferred over the entire silicon wafer area. The clear reproduction of the hole patterns in Si can also be seen in the SEM images of the master and the replicated structures, shown in the insets in figures 6(a) and 7(c).

To further demonstrate the flexibility of the SCIL technique we show that etch selectivity between silica and silicon can be used to invert the pattern tone. The SEM images and schematic cross sections insets shown in figure 7 illustrate an inversion of the hole pattern shown in figure 6. First, the hole pattern was imprinted in silica on a silicon wafer (a). Then the residual sol-gel resist layer was removed by CF_4 RIE and the pattern was transferred into the silicon substrate by Cl_2 RIE (b). The silica mask is removed by a wet HF etch, followed by spin-coating of a 100 nm thick sol-gel layer to planarize the surface. A CF_4 RIE is used to remove the residual sol-gel on

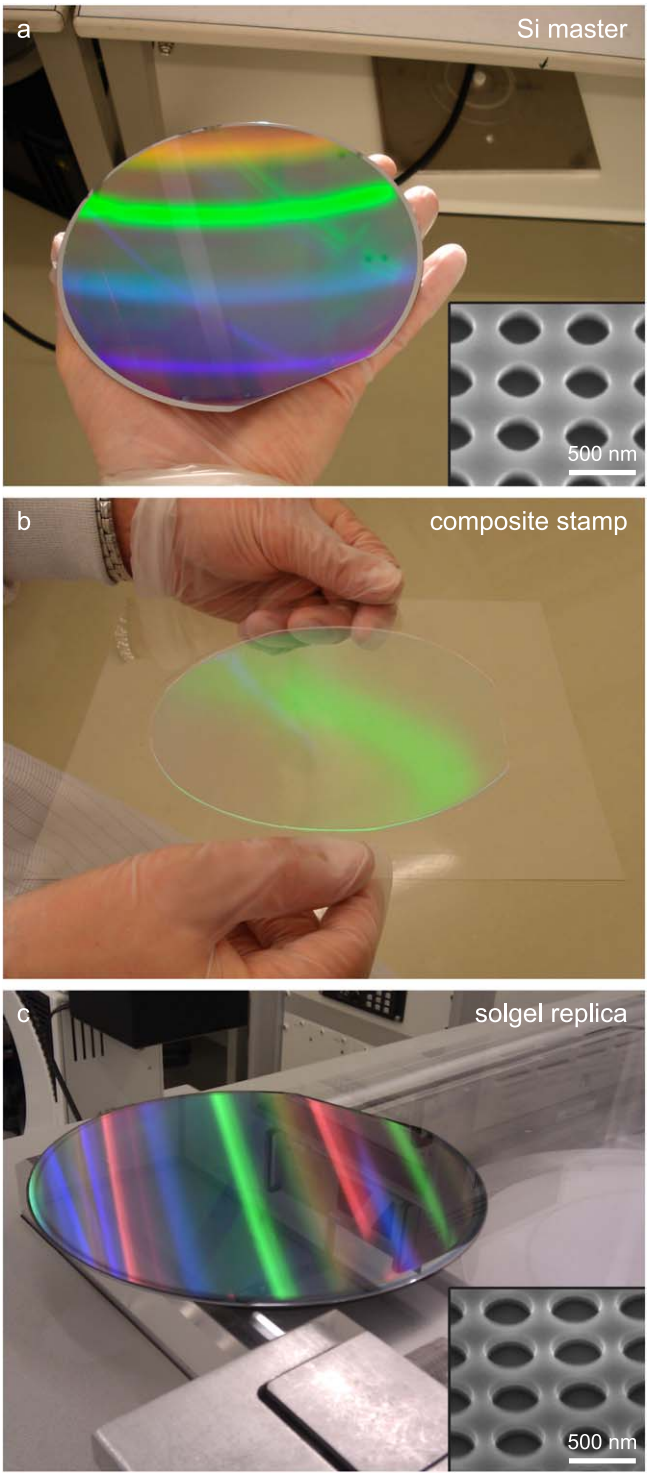

Figure 6. Wafer scale imprint and pattern transfer by SCIL. Uniform interference color bands in the (a) pattern master, (b) SCIL composite stamp, and (c) replicated pattern demonstrate the uniformity of a hole pattern (diameter 370 nm, pitch 513 nm) through the SCIL imprint process. The insets show SEM images of the structure (scale bar 500 nm).

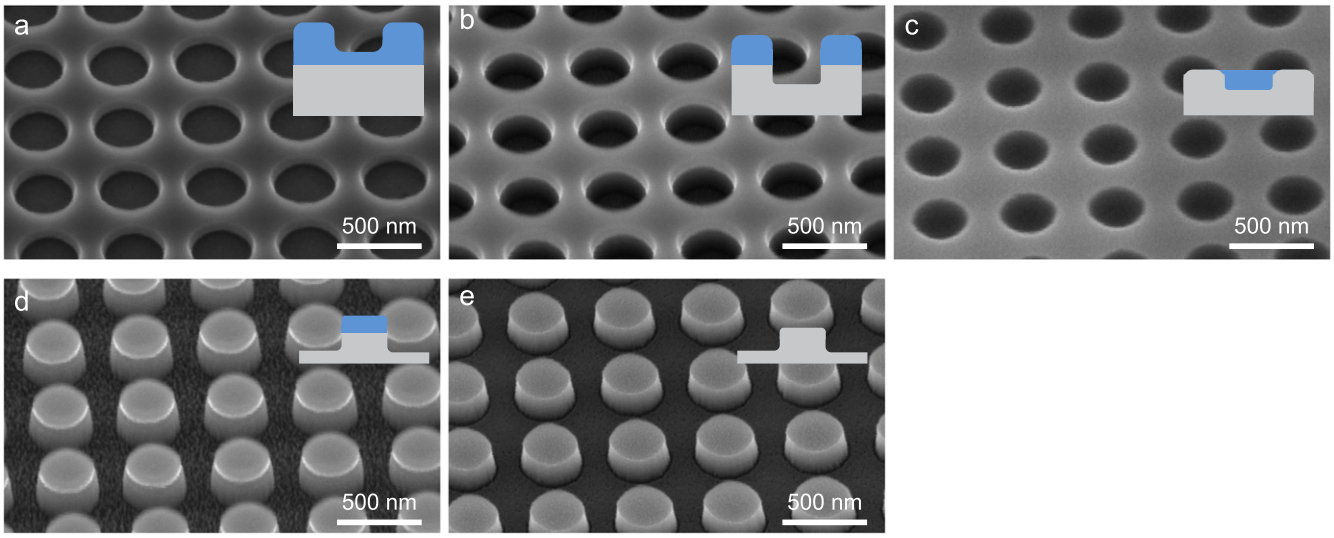

Figure 7. Pattern tone inversion using SCIL. A pattern of holes is imprinted in silica sol-gel resist on a silicon substrate (a) and transferred into the silicon by RIE (b). The silica etch mask is first removed by a wet etch before the hole patterns are planarized by a layer of spin coated sol-gel. This layer is subsequently RIE etched until the silicon is exposed between the silica filled holes (c) using a selective Cl_2/N_2 silicon etch the surrounding silicon is etched to below the silica plug, inverting the pattern tone (d) after which the silica dot mask is removed by a wet etch (e). This process inverts the hole pattern to a pillar pattern with equal fill fraction. Scale bars indicate 500 nm.

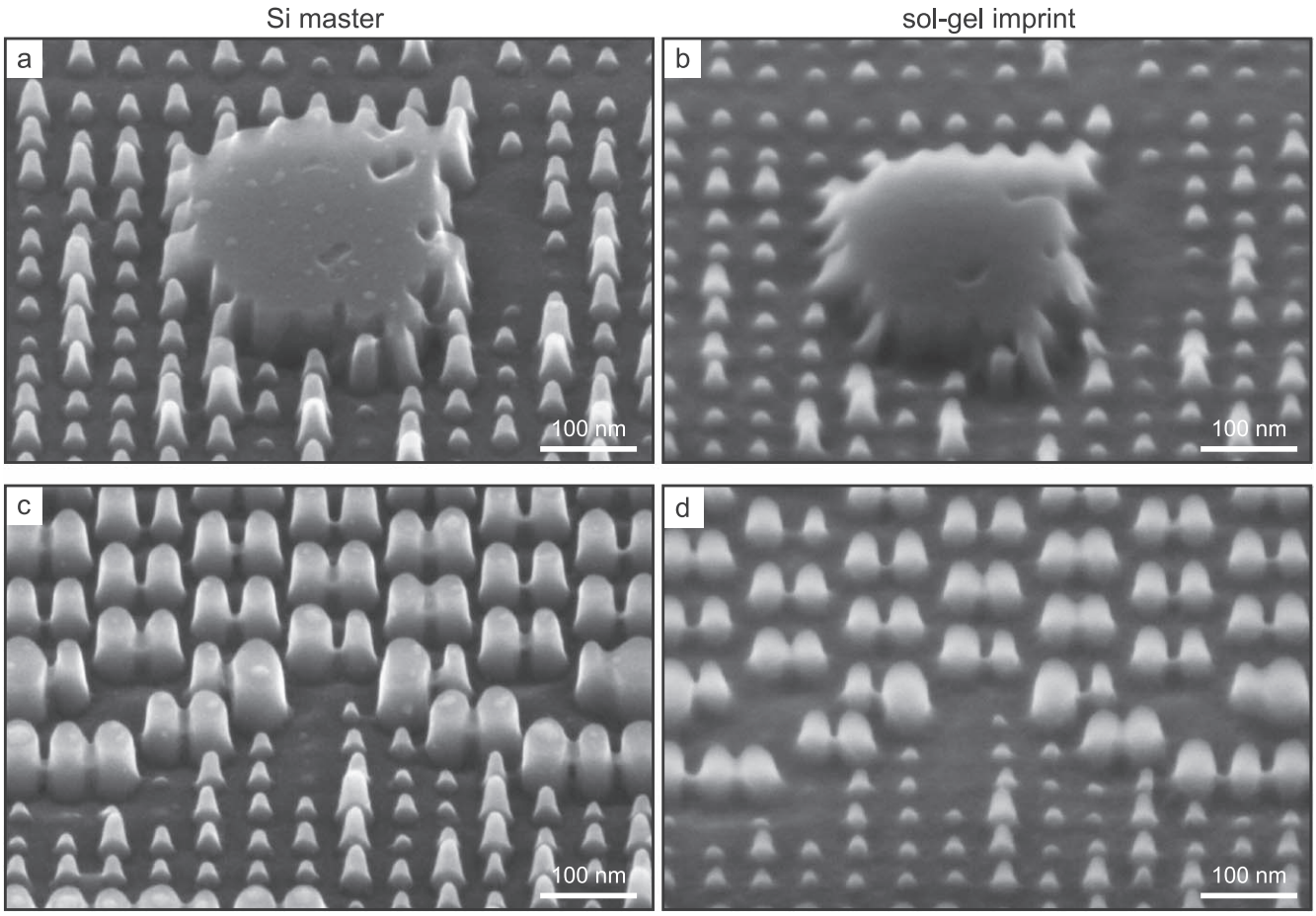

Figure 8. Direct comparison of Si master and sol-gel imprint. (a) Defect in the silicon master, (b) reproduction of this defect in cured sol-gel resist. (c) Pillars spaced ∼10 nm apart in the Si master and (d) identical area reproduced in sol-gel.

top of the surrounding silicon, leading to a planarized structure of holes in silicon that are filled, with sol-gel material (c). Next, the silicon surrounding the infilled holes is RIE etched using Cl_2 chemistry to below the depth of the holes to invert the pattern (d). A final wet HF etch removes the sol-gel etch mask (e). As can be seen in figure 7(e), a regular array of silicon pillars results with a fill fraction corresponding to the original hole pattern. The height of the pillars can be tuned by the duration of the final silicon RIE etch.

Finally, figure 8 provided a direct comparison between features in an etched Si master wafer and an exemplary solgel imprint made using a SCIL stamp fabricated from this master. Figure 8(a) shows a defect that had formed during the e-beam lithographic definition of a regular array of pillars in the Si master wafer. A defect was selected for this comparison due to the unique and easily identifiable geometry. The corresponding imprint in sol-gel, made using a PDMS stamp created from the Si master, is shown in figure 8(b). A comparison of the original Si feature with the imprinted solgel feature shows good correspondence. Similarly, we compare a geometry of differently shaped pillars in a master (figure 8(c)) and in the corresponding imprint in silica (figure 8(d)). Clearly, pillars that are only spaced 10 nm apart in the master are directly reproduced in the sol gel-based imprint resist.

5. Conclusions

We demonstrate a large-area substrate-conformal imprint lithography (SCIL) technique offering sub-10 nm resolution over 150 mm diameter substrates. A newly developed high-modulus X-PDMS stamp material enables the replication of dense nanoscale patterns while still allowing conformal contact across a full wafer. In-plane pattern distortions are avoided by lamination of the stamp to a thin glass carrier during stamp replication. The flexible composite stamp allows a novel silica based sol-gel imprint resist to be patterned with high fidelity. We demonstrate the direct replication of nanostructures with aspect ratios of up to 5:1, feature pitches as small as 30 nm, and a minimum feature size of 6 nm. The sol-gel resist exhibits low shrinkage and is light- and temperature-stable, which makes it appropriate for use as a directly patterned hard mask in subsequent RIE pattern transfer processes. We demonstrate the transfer of imprinted sol-gel patterns into silicon and silica by this method while preserving sub-10 nm resolution. By using the etch selectivity between the sol-gel imprint resist and silicon the imprinted patterns can be uniformly inverted at wafer scale.

Industrially, SCIL is already being applied to mass production of vertical-cavity surface-emitting lasers (VCSELs), where imprinted monolithic surface gratings enable polarization control [47]. Production data from 600 VCSEL wafers, processed in under a year using a single SCIL stamp, has demonstrated the self-cleaning nature of these stamps, and their resilience against surface contamination. Each wafer was inspected by AFM after breakthrough etching to measure the nanoscale feature dimensions; no degradation was observed across the production run.

In addition to this first application in VCSEL production, the SCIL process opens up many new possibilities in emerging application areas that rely on large-area nanopatterning, such as solid-state lighting, lasers, sensors, photovoltaics, meta-surfaces and optics for augmented reality applications.

Acknowledgments

The AMOLF contributions to this work are part of the research program of the Netherlands Organisation for Scientific Research (NWO). This research was supported by the Global Climate and Energy Program (GCEP) and the European Research Council (ERC) under the European Union's Horizon 2020 research and innovation programme (Grant agreement No. 695343).

ORCID iDs

M W Knight https://orcid.org/0000-0001-7625-403X
A Polman https://orcid.org/0000-0002-0685-3886

References

[1] Xia Y and Whitesides G M 1998 Soft Lithography *Annu. Rev. Mater. Sci.* **28** 153–84
[2] Schift H 2008 Nanoimprint lithography: an old story in modern times? A review *J. Vac. Sci. Technol.* B **26** 458–80
[3] Verschuuren M A, Megens M, Ni Y F, van Sprang H and Polman A 2017 Large area nanoimprint by substrate conformal imprint lithography (SCIL) *Adv. Opt. Technol.* **6** 243–64
[4] Wierer J J, Krames M R, Epler J E, Gardner N F, Craford M G, Wendt J R, Simmons J A and Sigalas M M 2004 InGaN/GaN quantum-well heterostructure light-emitting diodes employing photonic crystal structures *Appl. Phys. Lett.* **84** 3885–7
[5] Wierer J J, David A and Megens M M 2009 III-nitride photonic-crystal light-emitting diodes with high extraction efficiency *Nat. Photon.* **3** 163–9
[6] Altug H, Englund D and Vučković J 2006 Ultrafast photonic crystal nanocavity laser *Nat. Phys.* **2** 484–8
[7] Moore S A, O'Faolain L, White T P and Krauss T F 2008 Photonic crystal laser with mode selective mirrors *Opt. Express* **16** 1365–70
[8] Malyarchuk V, Hua F, Mack N, Velasquez V, White J, Nuzzo R and Rogers J 2005 High performance plasmonic crystal sensor formed by soft nanoimprint lithography *Opt. Express* **13** 5669–75
[9] McMahon J M, Henzie J, Odom T W, Schatz G C and Gray S K 2007 Tailoring the sensing capabilities of nanohole arrays in gold films with Rayleigh anomaly-surface plasmon polaritons *Opt. Express* **15** 18119–29
[10] Shir D, Yoon J, Chanda D, Ryu J H and Rogers J A 2010 Performance of ultrathin silicon solar microcells with nanostructures of relief formed by soft imprint lithography for broad band absorption enhancement *Nano Lett.* **10** 3041–6
[11] Soderstrom K, Escarre J, Cubero O, Haug F J, Perregaux S and Ballif C 2011 UV-nano-imprint lithography technique for the replication of back reflectors for n-i-p thin film silicon solar cells *Prog. Photovolt.* **19** 202–10

[12] Ferry V E, Verschuuren M A, Li H B, Verhagen E, Walters R J, Schropp R E, Atwater H A and Polman A 2010 Light trapping in ultrathin plasmonic solar cells *Opt. Express* **18** A237–45

[13] Chou S Y, Krauss P R and Renstrom P J 1996 Nanoimprint lithography *J. Vac. Sci. Technol.* B **14** 4129–33

[14] Haisma J, Verheijen M, vandenHeuvel K and vandenBerg J 1996 Mold-assisted nanolithography: a process for reliable pattern replication *J. Vac. Sci. Technol.* B **14** 4124–8

[15] Austin M D, Ge H X, Wu W, Li M T, Yu Z N, Wasserman D, Lyon S A and Chou S Y 2004 Fabrication of 5 nm linewidth and 14 nm pitch features by nanoimprint lithography *Appl. Phys. Lett.* **84** 5299–301

[16] Hua F, Gaur A, Sun Y, Word M, Jin N, Adesida I, Shim M, Shim A and Rogers J A 2006 Processing dependent behavior of soft imprint lithography on the 1–10 nm scale *IEEE Trans. Nanotechnol.* **5** 301–308

[17] Lin R and Rogers J A 2007 Molecular-scale soft imprint lithography for alignment layers in liquid crystal devices *Nano Lett.* **7** 1613–21

[18] Elhadj S, Rioux R M, Dickey M D, DeYoreo J J and Whitesides G M 2010 Subnanometer replica molding of molecular steps on ionic crystals *Nano Lett.* **10** 4140–5

[19] Tian C, Kim H, Sun W, Kim Y, Yin P and Liu H 2017 DNA nanostructures-mediated molecular imprinting lithography *ACS Nano* **11** 227–38

[20] Delamarche E, Schmid H, Michel B and Biebuyck H 1997 Stability of molded polydimethylsiloxane microstructures *Adv. Mater.* **9** 741–6

[21] Schmid H and Michel B 2000 Siloxane polymers for high-resolution, high-accuracy soft lithography *Macromolecules* **33** 3042–9

[22] Odom T W, Love J C, Wolfe D B, Paul K E and Whitesides G M 2002 Improved pattern transfer in soft lithography using composite stamps *Langmuir* **18** 5314–20

[23] Williams S S, Retterer S, Lopez R, Ruiz R, Samulski E T and DeSimone J M 2010 High-resolution PFPE-based molding techniques for nanofabrication of high-pattern density, sub-20 nm features: a fundamental materials approach *Nano Lett.* **10** 1421–8

[24] Chandra D and Yang S 2010 Stability of high-aspect-ratio micropillar arrays against adhesive and capillary forces *Acc. Chem. Res.* **43** 1080–91

[25] Xu B and Chen X 2011 Microfluidic channels formed by collapse of soft stamp *J. Nanomech. Micromech.* **1** 3–10

[26] Chandra D and Yang S 2009 Capillary-force-induced clustering of micropillar arrays: is it caused by isolated capillary bridges or by the lateral capillary meniscus interaction force? *Langmuir* **25** 10430–4

[27] Chandra D, Yang S, Soshinsky A A and Gambogi R J 2009 Biomimetic ultrathin whitening by capillary-force-induced random clustering of hydrogel micropillar arrays *ACS Appl. Mater. Interfaces* **1** 1698–704

[28] Zhao C, Xu X, Yang Q, Man T, Jonas S J, Schwartz J J, Andrews A M and Weiss P S 2017 Self-collapse lithography *Nano Lett.* **17** 5035–42

[29] Roy E, Kanamori Y, Belotti M and Chen Y 2005 Enhanced UV imprint ability with a tri-layer stamp configuration *Microelectron. Eng.* **78-79** 689–94

[30] Li Z, Gu Y, Wang L, Ge H, Wu W, Xia Q, Yuan C, Chen Y, Cui B and Williams R S 2009 Hybrid nanoimprint-soft lithography with sub-15 nm resolution *Nano Lett.* **9** 2306–10

[31] Chen L, Deng X G, Wang J, Takahashi K and Liu F 2005 Defect control in nanoimprint lithography *J. Vac. Sci. Technol.* B **23** 2933–8

[32] Schift H, Spreu C, Saidani M, Bednarzik M, Gobrecht J, Klukowska A, Reuther F, Gruetzner G and Solak H H 2009 Transparent hybrid polymer stamp copies with sub-50-nm resolution for thermal and UV-nanoimprint lithography *J. Vac. Sci. Technol.* B **27** 2846–9

[33] Perumal J, Yoon T H, Jang H S, Lee J J and Kim D P 2009 Adhesion force measurement between the stamp and the resin in ultraviolet nanoimprint lithography–an investigative approach *Nanotechnology* **20** 055704

[34] Gao H, Tan H, Zhang W, Morton K and Chou S Y 2006 Air cushion press for excellent uniformity, high yield, and fast nanoimprint across a 100 mm field *Nano Lett.* **6** 2438–41

[35] Truong T T, Lin R S, Jeon S, Lee H H, Maria J, Gaur A, Hua F, Meinel I and Rogers J A 2007 Soft lithography using acryloxy perfluoropolyether composite stamps *Langmuir* **23** 2898–905

[36] Campos L M, Truong T T, Shim D E, Dimitriou M D, Shir D, Meinel I, Gerbec J A, Hahn H T, Rogers J A and Hawker C J 2009 Applications of photocurable PMMS Thiol-Ene stamps in soft lithography *Chem. Mater.* **21** 5319–26

[37] Verschuuren M A 2010 Substrate conformal imprint lithography for nanophotonics *(PhD Thesis)* Utrecht University

[38] Jung G Y, Li Z, Wu W, Chen Y, Olynick D L, Wang S Y, Tong W M and Williams R S 2005 Vapor-phase self-assembled monolayer for improved mold release in nanoimprint lithography *Langmuir* **21** 1158–61

[39] Pina-Hernandez C, Kim J S, Guo L J and Fu P F 2007 High-throughput and etch-selective nanoimprinting and stamping based on fast-thermal-curing poly(dimethylsiloxane)s *Adv. Mater.* **19** 1222–7

[40] Plachetka U, Bender M, Fuchs A, Vratzov B, Glinsner T, Lindner F and Kurz H 2004 Wafer scale patterning by soft UV-nanoimprint lithography *Microelectron. Eng.* **73-4** 167–71

[41] Hong S H, Hwang J Y, Lee H, Lee H C and Choi K W 2009 UV nanoimprint using flexible polymer template and substrate *Microelectron. Eng.* **86** 295–8

[42] Verschuuren M A, McCoy J, Huber R P, Brakel R V, Paans M and Voorkamp R 2018 AutoSCIL 200mm tooling in production, x-ray optics, and cell growth templates *SPIE Proc Volume 10584, Novel Patterning Technologies* p 105840Z

[43] Fader R, Schmitt H, Rommel M, Bauer A J, Frey L, Ji R, Hornung M, Brehm M and Vogler M 2012 Novel organic polymer for UV-enhanced substrate conformal imprint lithography *Microelectron. Eng.* **98** 238–41

[44] Haslinger M J, Verschuuren M A, Brakel R V, Danzberger J, Bergmair I and Mühlberger M 2016 Stamp degradation for high volume UV enhanced substrate conformal imprint lithography (UV-SCIL) *Microelectron. Eng.* **153** 66–70

[45] Rogers J A, Paul K E and Whitesides G M 1998 Quantifying distortions in soft lithography *J. Vac. Sci. Technol.* B **16** 88–97

[46] Pagliara S, Persano L, Camposeo A, Cingolani R and Pisignano D 2007 Registration accuracy in multilevel soft lithography *Nanotechnology* **18** 175302

[47] Verschuuren M A, Gerlach P, van Sprang H A and Polman A 2011 Improved performance of polarization-stable VCSELs by monolithic sub-wavelength gratings produced by soft nano-imprint lithography *Nanotechnology* **22** 505201

[48] Verschuuren M A and Van Sprang H 2007 3D Photonic Structures by Sol-Gel Imprint Lithography *Proc. Mater. Res. Soc. Symp.* **1002** 1002-N03-05

[49] Marzolin C, Smith S P, Prentiss M and Whitesides G M 1998 Fabrication of glass microstructures by micro-molding of sol-gel precursors *Adv. Mater.* **10** 571–4

[50] Parashar V K, Styah A, Cuche E, Depeursinge C and Gijs M A M 2003 Diffractive optical elements in titanium oxide for MOEMS applications *Proc. IEEE Int. Conf. on Solid State Sensors, Actuators and Microsystems* vol 1482

[51] Li M, Tan H, Chen L, Wang J and Chou S Y 2003 Large area direct nanoimprinting of SiO2–TiO2 gel gratings for optical applications *J. Vac. Sci. Technol.* B **21** 660